Supplemental File S1

The 2023 State of the Climate Report: Entering Uncharted Territory

By William J. Ripple, Christopher Wolf, Jillian W. Gregg, Johan Rockström, Thomas M. Newsome, Beverly E. Law, Luiz Marques, Timothy M. Lenton, Chi Xu, Saleemul Huq, Leon Simons, Sir David Anthony King

Table of Contents

Supplemental Tables

Table S1. Summary of variables shown in Figures 2 and 3. Table columns show the variable name, update frequency, number of years with data, time of most recent data point, current value of the variable, change relative to the previous value, and rank (where rank 1 indicates the highest value to date). For variables with subannual frequency, the value, change, and rank are all based on year-to-date data. For example, they are based on the first 20.8% of each year for the variable "Carbon dioxide (CO_2 parts per million)" (since "Year" is equal to 2021.208). Note that variable time spans (# of years) differ significantly depending on the source. Variables that set all-time records are shown in red and marked with asterisks. Sources for these variables are given in this supplement.

Variable	Type	Years	Year	Value	Change	Rank
Human population (billion individuals)*	Annual	74	2023	8.05	0.0702	1
Total fertility rate (births per woman)*	Annual	62	2021	2.27	-0.0265	62
Ruminant livestock (billion individuals)*	Annual	61	2021	4.13	0.0255	1
Per capita meat production (kg/yr)*	Annual	61	2021	45.2	1.41	1
World GDP (trillion current US $/yr)*	Annual	64	2023	92.3	2.54	1
Global tree cover loss (million hectares/yr)	Annual	22	2022	22.8	-2.45	9
Brazilian Amazon forest loss (million hectares/yr)	Annual	35	2022	1.16	-0.147	22
Coal consumption (Exajoules/yr)	Annual	58	2022	161	1.04	2
Oil consumption (Exajoules/yr)	Annual	58	2022	191	5.83	3
Gas consumption (Exajoules/yr)	Annual	58	2022	142	-4.52	2
Solar/wind consumption (Exajoules/yr)*	Annual	58	2022	32.2	4.72	1

Air transport (billion passengers carried/yr)	Annual	49	2021	2.28	0.508	11
Total institutional assets divested (trillion USD)*	Annual	11	2022	39.2	24.5	1
CO_2e emissions (gigatonnes CO_2 equivalent/yr)*	Annual	33	2022	39.3	0.3	1
Per capita CO_2 emissions (tonnes CO_2 equivalent/yr)	Annual	33	2022	4.93	-0.00314	15
GHG emissions covered by carbon pricing (%)*	Annual	34	2023	23	0.69	1
Carbon price ($ per tonne CO_2 emissions)	Annual	34	2023	22.9	0.714	9
Fossil fuel subsidies (billion USD/yr)*	Annual	13	2022	1100	566	1
Governments that have declared a climate emergency (#)*	Annual	7	2022	2330	86	1
Carbon dioxide (CO_2 parts per million)*	Subannual	45	2023.458	420	2.03	1
Methane (CH_4 parts per billion)*	Subannual	40	2023.375	1920	13.2	1
Nitrous oxide (N_2O parts per billion)*	Subannual	46	2023.537	337	1.14	1
Surface temperature anomaly (change) (°C)	Subannual	144	2023.537	1.03	0.124	3
Earth's energy imbalance (W/m^2; 12-mo. running mean)*	Subannual	23	2023.452	1.73	0.187	1
Ocean heat content change (10^{22} joules)*	Annual	18	2022	28.2	0.912	1
Ocean acidity (pH)*	Subannual	34	2021.926	8.05	-0.0211	34
Sea level change relative to 20-year mean (mm)*	Subannual	31	2023.391	57.1	3.77	1
Minimum Arctic sea ice (million km^2)	Annual	44	2022	4.67	-0.05	34

Greenland ice mass change (gigatonnes)*	Subannual	22	2023.45	-5270	-167	22
Antarctica ice mass change (gigatonnes)	Subannual	22	2023.45	-2330	175	18
Glacier thickness change (m of water equivalent)*	Annual	73	2022	-26.7	-1.18	73
Area burned in the United States (million hectares/yr)	Annual	40	2022	3.07	0.183	11
Global tree cover loss due to fires (million hectares/yr)	Annual	22	2022	6.72	-2.62	8
Billion-dollar floods in the United States (events/year)	Annual	43	2022	1	-1	25
Extremely hot days relative to 1961–1990 (% of days/year)	Annual	72	2022	18.5	-0.65	3

Table S2. Regional summaries for 24 countries and The European Union. Variables shown are "CO_2e" (total CO_2 equivalent emissions associated with fossil fuel consumption in mega tonnes), "Population" (human population size in millions), "CO_2e/capita" (CO_2e emissions per capita in tonnes per person), "Share" (percentage of all CO_2e emissions associated with fossil fuel consumption compared to the global total), and "GDP/capita" (per capita gross domestic product in US dollars per person). All data are for the year 2022. Additional details on these variables are provided in the supplementary information below. GDP/capita was calculated using FAOSTAT population estimates and World Bank GDP estimates.

	CO_2e	Population	CO_2e/capita	Share	GDP/capita
China	11877	1458	8.1	30.4%	$12,321
United States	5298	338	15.7	13.6%	$75,269
India	2865	1417	2.0	7.3%	$2,389
The European Union	2709	447	6.1	6.9%	$37,203
Russia	2024	145	14.0	5.2%	$15,482
Japan	1093	124	8.8	2.8%	$34,135
Iran	905	89	10.2	2.3%	$4,388
Indonesia	840	276	3.0	2.2%	$4,788
Saudi Arabia	724	36	19.9	1.9%	$30,436
South Korea	618	52	11.9	1.6%	$32,138
Canada	591	38	15.4	1.5%	$55,646
Mexico	578	128	4.5	1.5%	$11,091
Brazil	506	215	2.4	1.3%	$8,918
South Africa	456	60	7.6	1.2%	$6,776
Turkey	453	85	5.3	1.2%	$10,616
Australia	437	26	16.7	1.1%	$64,002
United Kingdom	355	68	5.3	0.9%	$45,485
Vietnam	353	98	3.6	0.9%	$4,164
United Arab Emirates	328	9	34.7	0.8%	$53,758
Iraq	315	44	7.1	0.8%	$5,937
Thailand	307	72	4.3	0.8%	$6,909
Malaysia	299	34	8.8	0.8%	$11,972

Kazakhstan	287	19	14.8	0.7%	$11,373
Egypt	284	111	2.6	0.7%	$4,295
Algeria	246	45	5.5	0.6%	$4,274
Top 25	**34747**	**5435**	**6.4**	**89.1%**	**$16,359**
World	**39316**	**7975**	**4.9**	**100.0%**	**$11,255**

Supplemental Figures

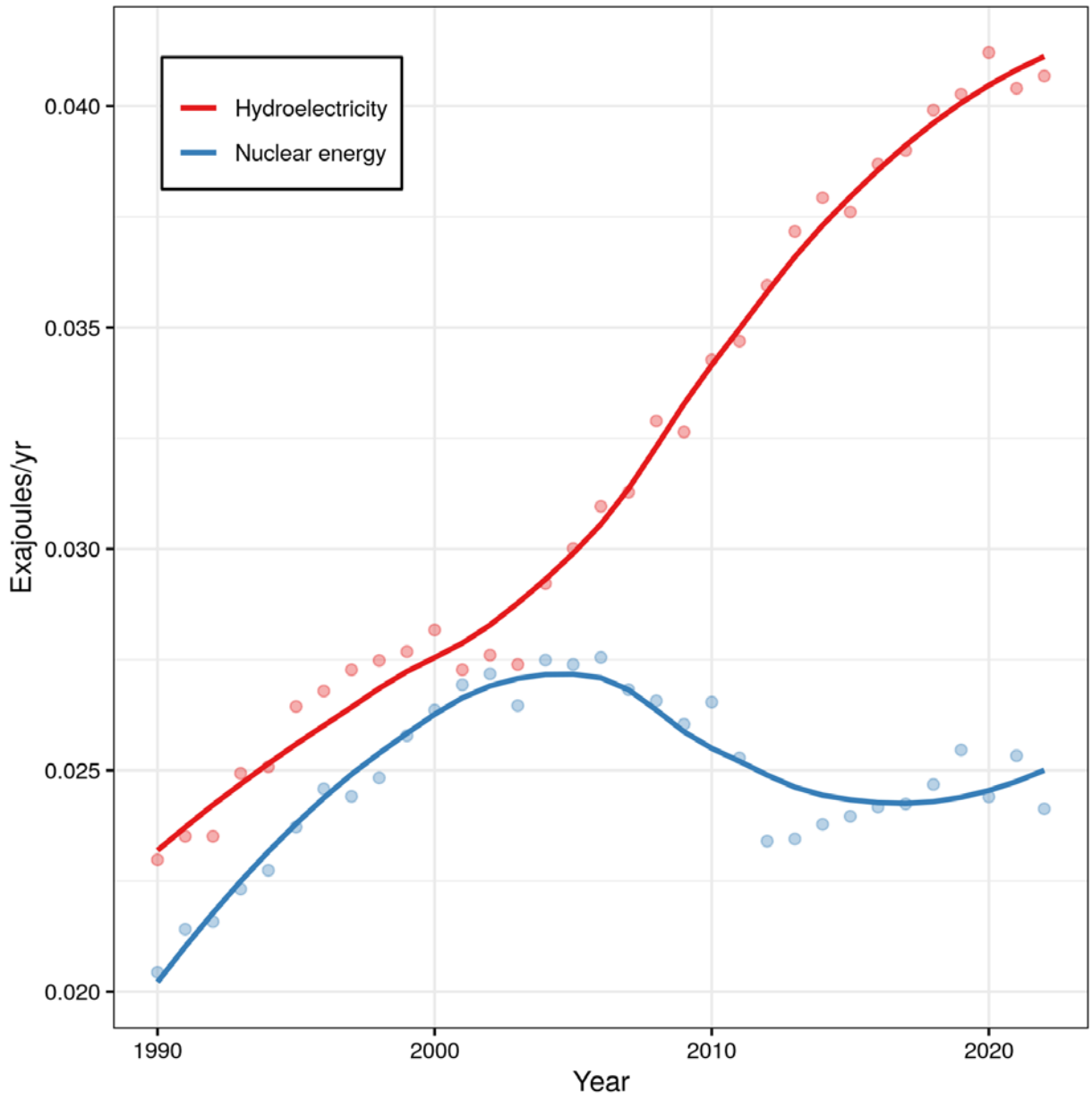

Figure S1. Annual consumption rates for nuclear energy and hydroelectricity (British Petroleum Company 2022). Non-fossil fuel energy supply pathways in the future may include hydro and nuclear power in addition to wind and solar power (IPCC 2018). See British Petroleum Company (2022) for other minor energy sources not shown in this figure. Figure 2h in the main text shows consumption of fossil fuels as well as solar/wind energy.

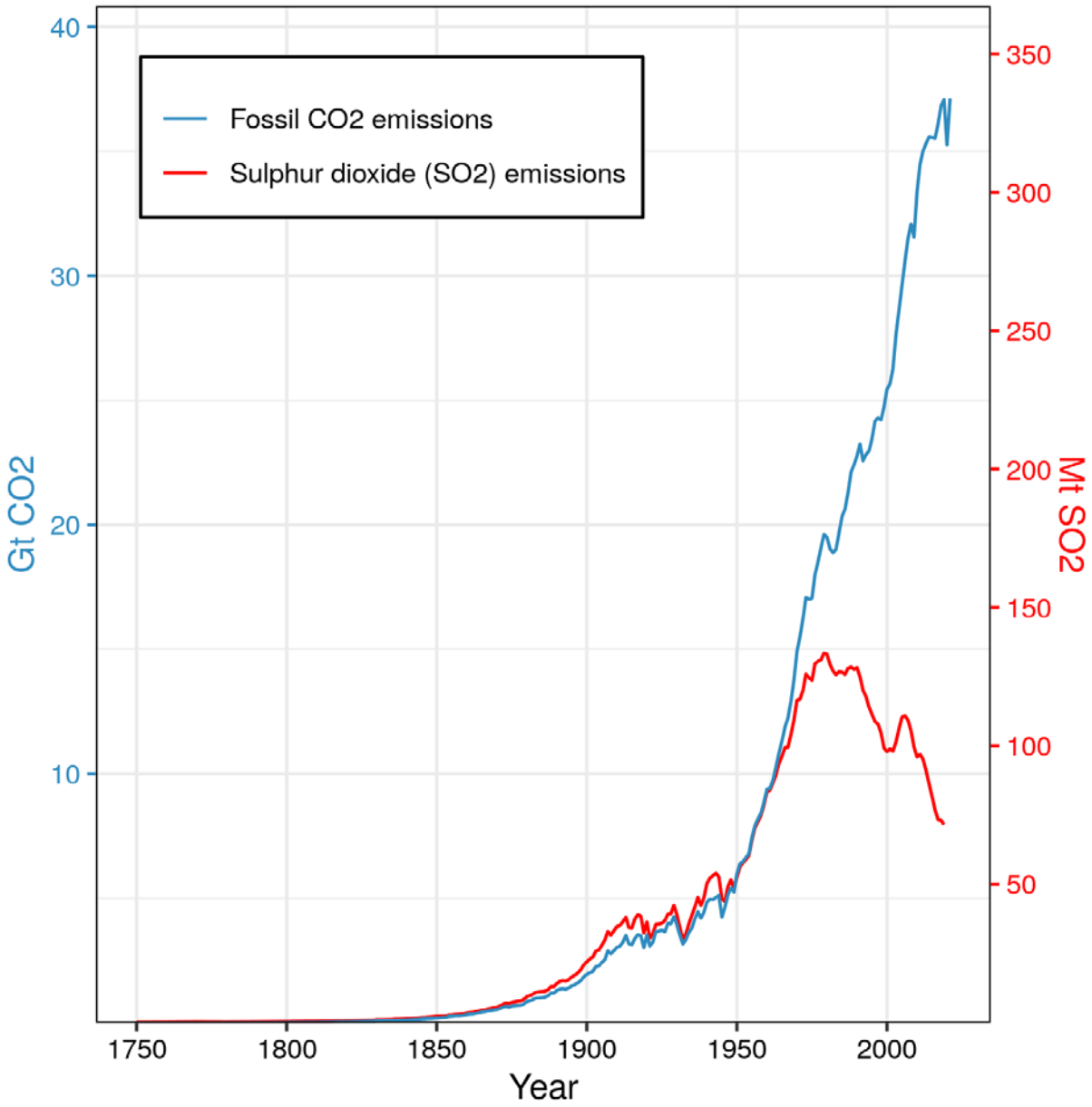

Figure S2. Global anthropogenic emissions of sulfur dioxide (SO_2) and fossil fuel emissions of carbon dioxide (CO_2; excluding carbonation). SO_2 is an air pollutant that can form acid rain, but which also has a cooling effect. SO_2 estimates come from O'Rourke et al. (2021), are described in Hoesly et al. (2018), and were downloaded from Our World in Data (2023). CO_2 estimates come from the 2022 Global Carbon Budget (Friedlingstein et al. 2022).

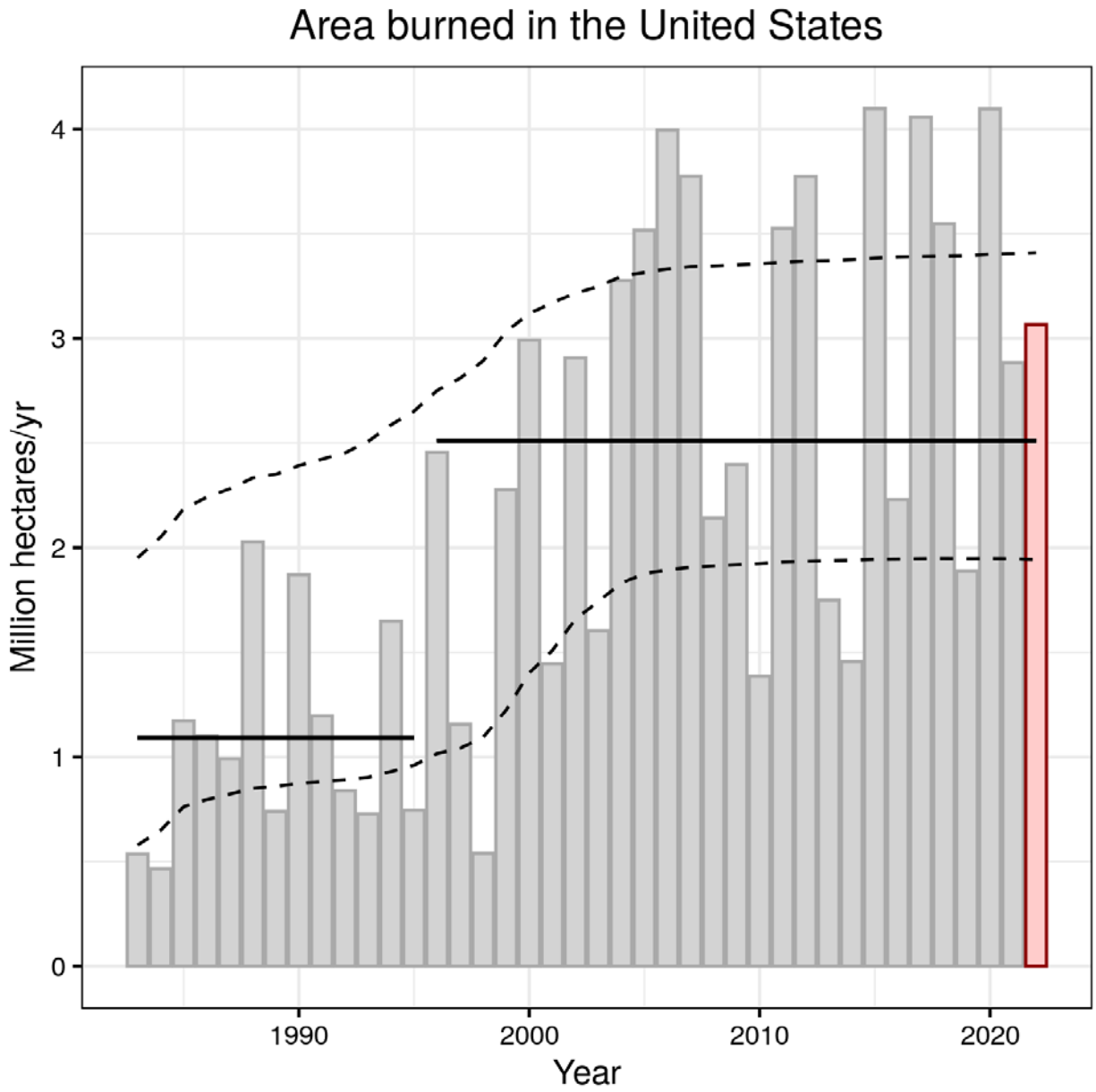

Figure S3. Approximate area burned in the U.S. (see figure 3m). The solid black lines show the predicted mean area burned according to a Bayesian change-point regression model. The dashed black lines correspond to an 80% credible band. According to this model, a new fire regime began around 1996 [80% credible interval: (1985, 2004)], although more research is needed to support this finding. Weakly informative priors were used for the rate parameters and inference was based on 8,000 posterior samples (see Supplementary Methods).

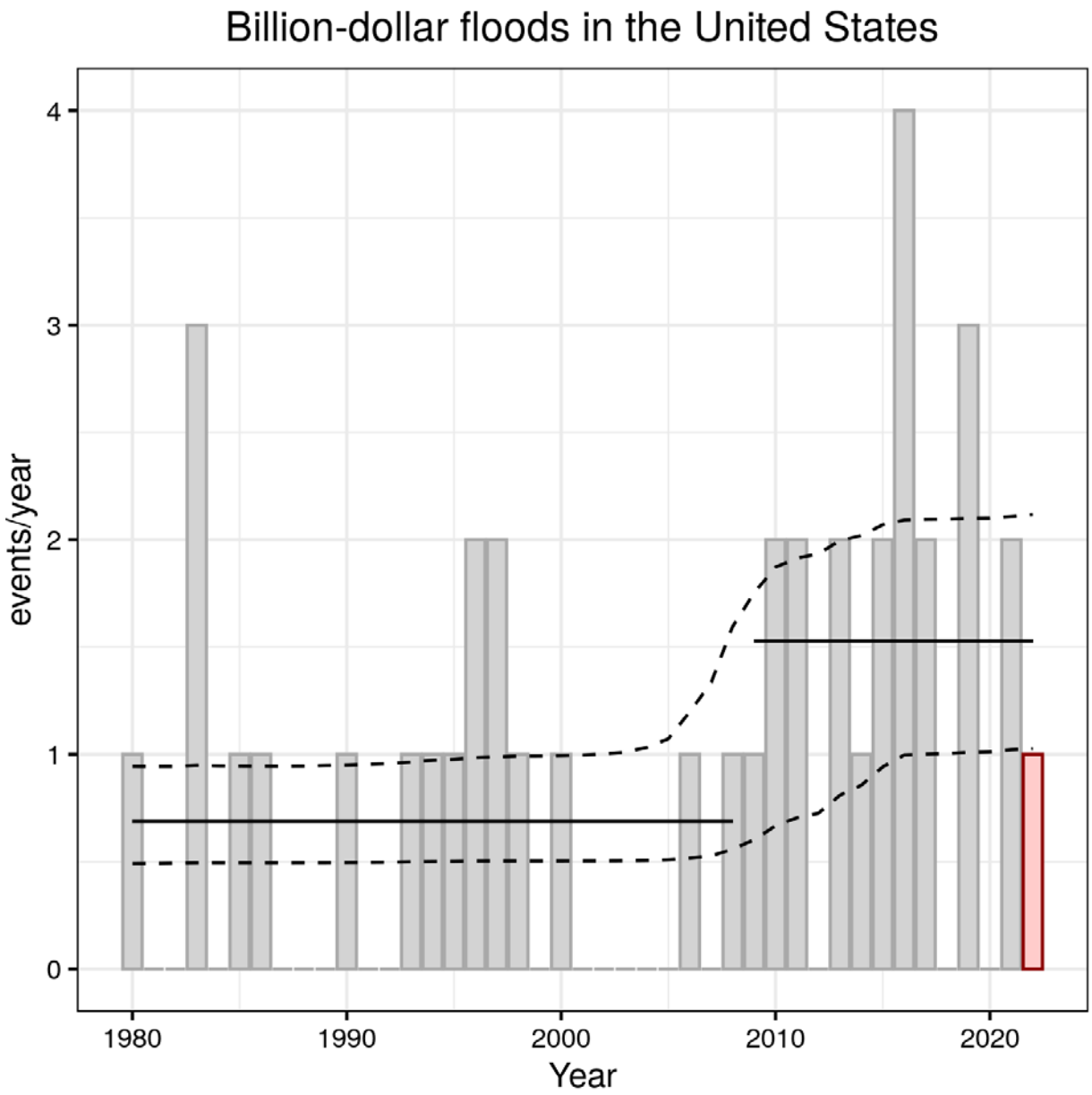

Figure S4. Number of inflation-adjusted billion-dollar floods in the U.S. (see figure 3o). The solid black lines show the predicted mean number of floods according to a Bayesian change-point regression model. The dashed black lines correspond to an 80% credible band. According to this model, a new flood regime began around 2009 [80% credible interval: (1996, 2015)], although more research is needed to support this finding. Weakly informative priors were used for the rate parameters and inference was based on 8,000 posterior samples (see Supplementary Methods).

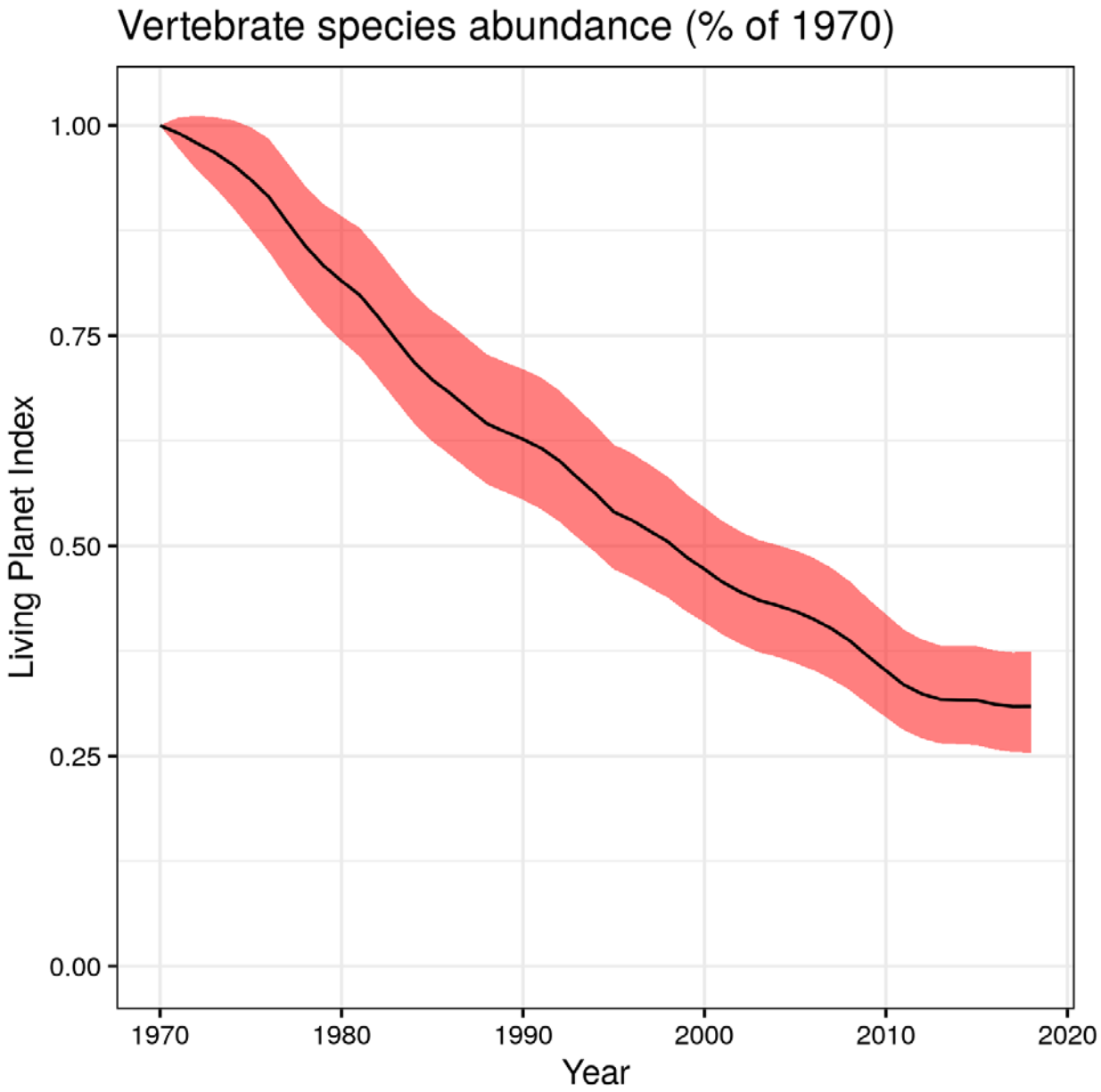

Figure S5. Trends in global vertebrate species abundance according to the Living Planet Index (WWF 2022). This index is a biodiversity indicator that tracks the relative abundance of wild vertebrate species since 1970 (WWF 2022). It is derived from tens of thousands of abundance time series for terrestrial, freshwater, and marine vertebrate species populations (Loh et al. 2005, Collen et al. 2009, McRae et al. 2017). The red band corresponds to a 95% confidence interval. As of 2018, the value of the index is 0.31, corresponding to a 69% decline.

Climate Impacts: Untold Human Suffering in Pictures

Here, we present a compilation of photographs intended as a visual demonstration of the recent impacts of climate change. Photos generally show human suffering due to natural disasters that may be at least partly attributable to climate change. The photos primarily come from the last decade (2013-2022) and are grouped into two themes: flooding and drought.

All photos are Creative Commons licensed or Public Domain and most were obtained through the Climate Visuals project (https://climatevisuals.org/), which compiles images from many sources. Specific credits are given with each image along with a brief description of the event. All quotations describing images are from the Climate Visuals project.

Mozambique, 2019. “Aftermath of Cyclone Idai.” Credit: Denis Onyodi: IFRC/DRK/Climate Centre, CC BY-NC 2.0.

United States, 2008. Homeowners sort through debris after wildfires destroyed their home in the state of California. Credit: FEMA/Michael Mancino, Public Domain.

Sri Lanka, 2010. “Heavy monsoon showers inundated the roads in Dharga Town.” Credit: Hafiz Issadeen, CC BY 2.0.

Brazil, 2015. “Mature woman seated in her home, submerged in deep water, smoking a cigarette [...].” Credit: Fabrice Fabola, CC BY-SA 2.0.

United States, 2017. “[National] Guardsman giving a woman a piggyback in waist deep floodwaters outside a house, Texas National Guard soldiers conduct rescue operations in flooded areas around Houston, Texas.” Credit: Zachary West / National Guard, CC BY 2.0.

The Philippines, 2013. “Residents walk on a road littered with debris after Super Typhoon Haiyan battered Tacloban city in central Philippines.” Credit: Erik de Castro / Reuters, CC BY 2.0.

United States, 2013. “Flooding and water damage in the Park and Tongue River Watersheds located in Cavalier, Pembina and Cavalier Counties in [North Dakota].” Credit: USDA, CC BY 2.0.

South Sudan, 2014. “Two small boys wading through water in a rural landscape, a flood plain.” Credit: JC Mcllwaine / UNMISS, Creative Commons

United Kingdom, 2014. “Man wades through flooded Cornish high street in the village of Fowey.” Credit: Prawny / Pixabay, Creative Commons.

Afghanistan, 2019. “In the Afghan city of Bamiyan, young girls are caught by a sandstorm on their way to school.” Credit: Solmaz Daryani / Climate Visuals Countdown, Creative Commons

Mozambique, 2019. “Two young people carrying large electrical goods through flood waters, amplifiers.” Credit: Denis Onyodi / IFRC/DRK, CC BY-NC 2.0.

Recent climate-related disasters (Table 1)

Below, we list numerous recent disasters that may be at least partly related to climate change. This list is not intended to be exhaustive. Due to the recent nature of these events, our sources often include news media articles. We have considered only disasters that occurred after the most recent disaster listed in our previous year's report (i.e., after October, 2022).

Because of the natural variability and stochasticity of the Earth system, attributing specific extreme events (or parts of their impacts) to climate change is an exceptionally challenging task (Stott et al. 2013, Trenberth et al. 2015), although it may be possible in some cases (e.g., Strauss et al. 2021). For simplicity, we have generally adopted the framework of Stott et al. (2013), which is described by Trenberth et al. (2015 p. 725) as follows:

"[T]he approach is to characterize the event and ask (i) whether the likelihood or strength of such events has changed in the observational record, and (ii) whether this change is consistent with the anthropogenic influence as found in one or more climate models, and thereby assess the 'fraction of attributable risk'."

Thus, for each event, we provide references indicating that the likelihood or strength of such an event may have become more common due to anthropogenic climate change. For certain types of events (e.g., rainfall), this can be difficult to establish conclusively. Because of this potential issue, we have indicated cases where attribution (in the general sense described above) has a high degree of uncertainty. Since our intention is to provide a brief overview of potentially climate related disasters, we have opted not to assess the "fraction of attributable risk" for each event.

Note that some of these climate disasters may be at least partly related to changes in jet streams (Stendel et al. 2021, Rousi et al. 2022).

1. (November–December 2022) Record-breaking heat waves in Argentina and Paraguay contributed to power outages, wildfires, and poor harvests. This extreme heat was estimated to have been made 60 times more likely due to climate change.
2. (December 2022–March 2023) Heavy rainfall caused by atmospheric rivers led to multiple floods in the Western United States. There were at least 22 fatalities and property damages were estimated to be 3.5 billion US dollars. Climate change may be increasing the likelihood of such catastrophic floods, although its effect on these particular storms is less clear.
3. (February 2023) Cyclone Gabrielle caused extreme rainfall in Aotearoa New Zealand's Te Ika-a-Māui (North Island), potentially resulting in billions of dollars in damages and 225,000 homes losing power. This intense rainfall may be partly caused by a warming climate.

4. (March–May 2023) Record-breaking temperatures were recorded in parts of Southeast Asia, China, and South Asia. The extreme heat caused deaths and school closures in India and led to more than 100 students requiring treatment for dehydration in the Philippines. It was likely at least partly due to climate change. For example, climate change has increased the likelihood of such an event to occur over Bangladesh and India by a factor of at least 30.
5. (January–July 2023) Intense wildfires in Canada burned roughly 10 million hectares, displacing 30,000 people at their peak, and worsening air quality across large portions of Canada and the United States. These extreme wildfires may be partly due to climate change, although many other factors are likely involved.
6. (May 2023) Tropical cyclone Mocha is reported to have killed at least 145 people in Myanmar and affected roughly 800,000 people in the region. Climate change may have made such storms more intense.
7. (May–June 2023) Tropical storm Mawar caused flooding and loss of power in parts of Guam. Mawar is the strongest cyclone ever recorded in the northern hemisphere in May. Climate change may be causing an increase in the intensity of tropical cyclones (Wu et al. 2022).
8. (June 2023) Deadly heat led to more than a dozen deaths in the Southern and Midwestern United States. Climate change is leading to an increase in the frequency and duration of such heat waves.
9. (July 2023) Up to six people died in Southwest Japan due to extremely heavy rainfall that caused floods and landslides. Climate change is likely making such heavy rainfall events more severe. Days later, floods and landslides, which may have been partly climate change-related, killed more than 26 people and led to thousands being evacuated in South Korea
10. (July 2023) Heavy monsoon rain caused flash floods and landslides in Northern India that killed more than 100 people. Climate change is likely making monsoons in this region more variable, causing frequent landslides and floods. Heavy monsoon rains also damaged rice crops in India, raising concerns about global food prices and food security and prompting an export ban on non-basmati varieties.
11. (June–August 2023) Extreme heat in the United States killed at least 147 people. In the absence of climate change, the extreme heat seen in July 2023 in the United States would have been extremely unlikely to occur.
12. (July–August 2023) Beijing, China experienced its heaviest rainfall in at least 140 years, resulting in major flooding that affected nearly 1.29 million people, damaged 147,000 homes, and caused at least 33 deaths. Intense flooding is likely becoming more common due to climate change.
13. (August 2023) In Hawaii, United States, catastrophic wildfires on the island of Maui killed at least 111 people, with more than 1,000 people likely missing, as of August

18, 2023. Climate change may have decreased rainfall and increased temperatures in this region, potentially contributing to these fires.

14. (September 2023) Storm Daniel caused extreme flooding in Libya and parts of southeastern Europe, resulting in thousands of fatalities and more than US$2 billion in damages. Climate change may be increasing the intensity of such storms.

Increased warming from reduced sulfur pollution

The current warming of our planet is mainly driven by the increased concentration of greenhouse gases in the atmosphere. The main source of increased greenhouse gas emissions is the burning of fossil fuels (IPCC 2021).

It has long been known that the sulfur from fossil fuels released in the atmosphere causes temporary regional cooling and less global warming (Hansen and Lacis 1990). The IPCC estimated that SO_2 emissions cooled the climate by about -0.5 C (-0.1 to -0.9 C) up to 2019 (IPCC 2021). The formed sulphate aerosols reflect sunlight and act as Cloud Condensation Nuclei, forming clouds and making existing clouds more reflective, larger, and longer lasting (IPCC 2021). Recent observational research shows that this effect was likely stronger than initially thought, especially over the oceans (Wall et al. 2022).

As we are now using cleaner fuels (e.g., increasing natural gas over coal; use of less sulfur-rich oil, and filters scrubbing SOx emissions from smokestacks), the rate of warming is increasing, especially in regions where emissions are reduced (Cherian et al. 2014, Zheng et al. 2020, Forster et al. 2023). In 2020, international shipping SOx emissions decreased by about 80% in response to new International Maritime Organization sulfur regulations (Hausfather and Forster 2023). These changes coincided with regional and global decreases in reflected sunlight (albedo), more solar heat being absorbed, and with an increase in Earth's Energy Imbalance (Figure 3e; Loeb et al. 2021, Hansen et al. 2022, Diamond 2023).

More research on aerosol-related climate and weather impacts is needed with a focus on attribution and better quantifying present and future risks (Persad et al. 2022). Note that aerosol changes can also impact regional precipitation and cause changes in ocean and atmospheric currents (Salzmann 2016, Zhao and Suzuki 2021, Dong et al. 2022).

Anomalies in 2023 (Figure 1)

Sea ice extent (Figure 1 a,b)

Antarctic and global sea ice extent data come from the "VIsualization Service of Horizontal scale Observations at Polar region" website; see their "Method for calculating sea-ice extent" section for details (VISHOP 2023).

Temperatures (Figure 1 c–e)

Ocean temperature anomaly data come from the Climate Reanalyzer website (Birkel 2023) and are derived from the "NOAA OISST V2.1" dataset (Huang et al. 2021).

Global temperature data also come from Climate Reanalyzer and are derived from the "NCEP CFSV2/CFSR" dataset (Saha et al. 2014). We adjusted these data to the 1850–1900 reference level by first subtracting the 1991–2020 mean (separately for each day) and then adding 0.88 C (Copernicus 2023).

Area burned in Canada (Figure 1f)

Data on cumulative total area burned by wildfires in Canada are from the Canadian Wildland Fire Information System's Fire M3 Hotspots "Season-to-date Hotspot Reports" (Natural Resources Canada 2023).

Methods for planetary vital signs

Ripple et al. (2020) compiled a set of global time series related to human actions that affect the environment and climate (e.g. fossil fuel consumption) and the associated environmental and climatic responses (e.g. temperature change). We have made a number of updates to this set of variables, which are described below. For completeness, we also describe all relevant methods, variables, and sources in full here, but note that there may be some overlap with Ripple et al. (2020) given the nature of this update.

Although the data used are from sources believed to be reliable, no formal accuracy assessment for these datasets has been made by us and users should proceed with caution. With the exception of climate emergency declarations (see next section), all the "human actions" time series are annual. However, many of the "environmental and climatic responses" time series are subannual (e.g., monthly). In contrast to Ripple et al. (2020), we opted to keep these eight time series at their original (source) frequency rather than resampling to annual frequency.

For each variable, we calculated the following statistics:

1. The number of years with data (e.g., a variable with data from 1960 to 2021 would have 62 years of data)
2. The most recent year with data (can be fractional for subannual frequency variables – for example, 2021.35)
3. The most recent value of the variable (year-to-date average for subannual variables)
4. The most recent change in the variable (between current and preceding year-to-date averages for subannual variables)
5. The rank associated with the most recent value (#3) based on the entire time series. For example, a rank of 2 means the variable is at its second highest level ever (second highest year-to-date average for subannual variables).

While we only plotted data between 2000 and the present (2021), we included data from before 2000 (if available) when calculating the above statistics.

Models for vital signs

For area burned in the United States and billion-dollar floods in the United States, we fitted Bayesian changepoint models to explore the possibility of abrupt shifts in these time series. Following Fonnesbeck et al. (2017), we treated the number of billion dollar floods in each year as Poisson distributed, with two rate parameters—one before the breakpoint and another after the breakpoint. We treated the breakpoint location itself as a latent discrete parameter, with a discrete uniform prior. For the rate parameter priors, we used weakly informative exponential

distributions with mean 10 (and variance 100). We used the same approach to model area burned, except we treated the data as following exponential distributions, rather than Poisson distributions.

We marginalized out the latent discrete breakpoint parameters and fit the models using the Stan probabilistic programming language (Carpenter et al. 2017). We based inference on 8,000 MCMC posterior samples (from 4 chains with 2,000 burnin samples discarded per chain). It is important to note that this analysis was intended as a simple and preliminary assessment of possible abrupt shifts in certain climate-related disaster variables. To make rigorous conclusions, further research is needed. For example, followup work could consider more flexible probability distributions, account for possible temporal autocorrelation, or incorporate climate-related predictor variables

For the plots of the other “environmental and climatic responses” variables with high variance, we included smooth trend lines calculated using locally estimated scatterplot smoothing. We fit the trend lines in R using the ‘loess’ function with default settings (degree 2, span 0.75) (R Core Team 2018).

Indicators of climate-related human activities (Figure 2)

Below, we list sources and provide brief descriptions of indicators used in our analysis. Full methods for each indicator are available at the provided sources.

Human population (Figure 2a)

We used the Food and Agriculture Organization Corporate Statistical Database (FAOSTAT) as our source of human population data (FAOSTAT 2023). For human population estimates, the source data used by FAOSTAT are derived from national population censuses. For 2019 through 2022, these estimates are classified as "year projections."

Total fertility rate (Figure 2b)

We obtained this variable from the World Bank (The World Bank 2023a). The full variable name is "Fertility rate, total (births per woman)" and the World Bank variables ID is SP.DYN.TFRT.IN. This variable was derived using data from multiple sources, including the United Nations Population Division. The full list of original sources is available at The World Bank (2023a). Total fertility rate is defined as "the number of children that would be born to a woman if she were to live to the end of her childbearing years and bear children in accordance with age-specific fertility rates of the specified year" (The World Bank 2023a).

Ruminant livestock population (Figure 2c)

We used the Food and Agriculture Organization Corporate Statistical Database (FAOSTAT) as our source of ruminant livestock population data (FAOSTAT 2023). We considered ruminants to be members of the following groups: cattle, buffaloes, sheep, and goats. For livestock estimates, the primary data sources are national statistics obtained using questionnaires or collected from countries' websites or reports. When national livestock statistics were unavailable, they were estimated by FAOSTAT using imputation (FAOSTAT 2023).

Per capita meat production (Figure 2d)

We used total meat production data from FAOSTAT along with FAOSTAT human population size estimates (figure 2a) to estimate per capita meat production (FAOSTAT 2023). The meat production estimates are for the "Meat, Total" item under the "Crops and livestock products" domain (FAOSTAT 2023).

World gross domestic product (Figure 2e)

We obtained this variable from the World Bank (2023b) for the years 1960 to 2021. The full variable name is "GDP (constant 2015 US$)" and the World Bank variable ID is

NY.GDP.MKTP.KD. This variable was derived from multiple sources such as World Bank national accounts. For details, including limitations and exceptions, see The World Bank (2023b). Gross domestic product (at purchaser's prices) is defined as "the sum of gross value added by all resident producers in the economy plus any product taxes and minus any subsidies not included in the value of the products" (The World Bank 2023b).

We calculated a projection for 2022 gross domestic product (GDP) using the April 2022 edition of the International Monetary Fund's World Economic Outlook Database (IMF 2022). We first obtained the year 2022 percentage change estimate based on the variable "Gross domestic product, constant prices" in units "Percent change" (IMF 2022). We then used this percentage change estimate to predict total GDP (as measured by the World Bank in constant 2015 US dollars) in 2022. Because IMF projections and World Bank and World Economic Outlook GDP estimates likely differ in methodology, this 2022 estimate should only be considered an approximation.

Global tree cover loss (Figure 2f)

We obtained data on annual global tree cover loss from Global Forest Watch (Hansen et al. 2013). These data express loss globally in million hectares (Mha) and were derived from remotely-sensed forest change maps. It should be noted that loss is general and not linked to a specific type of deforestation. So, it includes wildlife, conversion to agriculture, disease, etc. Additionally, tree cover loss does not take tree cover gain into account. Thus, net forest loss may be lower than the reported numbers.

Some of the apparent variation in loss rates may be due to non-forest factors such as changes in the modeling algorithm, satellite data quality, and satellite data variability (Global Forest Watch 2022). Thus, trends in tree cover loss rates should be interpreted with this limitation in mind.

Brazilian Amazon forest loss (Figure 2g)

We obtained annual Brazilian Amazon forest loss estimates from Butler (2023). Brazil contains about 60% of the Amazon rainforest. We used annual deforestation estimates rather than monthly ones because of high month-to-month variability. Due to cloud cover issues, each annual estimate is for the period August 1 to July 31. For example, the 2021 estimate is for deforestation occurring between August 1, 2020 and July 31, 2021.

The original source of these data is PRODES — the annual deforestation monitoring system of Brazil's National Institute for Space Research (INPE). PRODES deforestation estimates are based on remotely sensed Landsat-type data.

Energy consumption (Figure 2h)

We used the Energy Institute's 2023 Statistical Review of World Energy as our primary source of data on energy consumption (The Energy Institute 2023). For energy consumption, we used the following time series: coal, oil, natural gas, solar, and wind. We grouped solar and wind together into a single category. Coal consumption data are only for commercial solid fuels. In each case, the units of energy consumption are exajoules (per year). Other sources of low carbon energy such as hydropower and nuclear power are shown in figure S1.

Air transport (Figure 2i)

We obtained estimates from the World Bank (The World Bank 2023c). The full variable name is "Air transport, passengers carried." The corresponding World Bank variable ID is IS.AIR.PSGR. This variable was derived from multiple sources, including the International Civil Aviation Organization. The full list of sources is available at The World Bank (2023c). Air transport includes both domestic and international travelers.

Divestment (Figure 2j)

Divestment data were obtained from 350.org (350.org 2021; Fossil Free 2021). They cover institutional divestment by 1,117 organizations. The most commonly represented institutions were faith-based organizations, philanthropic foundations, educational institutions, governments, and pension funds (Fossil Free 2021). Using 350.org's divestment database, we calculated cumulative total institutional divestment by year (since 2013) based on the "date of record" variable, which "generally represents the organization's divestment commitment announcement date" (350.org 2021).

Note that more sophisticated metrics are needed to determine which companies should be subject to divestment (Mormann 2020).

CO_2 emissions (Figure 2k)

We used the Energy Institute's 2023 Statistical Review of World Energy as our source of data on CO_2 emissions (The Energy Institute 2023). Specifically, we used the variable "Carbon Dioxide Equivalent Emissions from Energy, Process Emissions, Methane, and Flaring," which is defined as "the sum of carbon dioxide emissions from energy, carbon dioxide emissions from flaring, methane emissions, in carbon dioxide equivalent, associated with the production, transportation and distribution of fossil fuels, and carbon dioxide emissions from industrial processes" (British Petroleum Company 2022).

Per capita CO_2 emissions (Figure 2l)

We converted total CO_2 emissions (figure 2k) to per capita CO_2 emissions using FAOSTAT human population size estimates (figure 2a).

Greenhouse gas emissions covered by carbon pricing (Figure 2m)

The data on percentage of greenhouse gas emissions covered by carbon pricing schemes are taken directly from World Bank Group (2023). When multiple schemes covered the same emissions, the emissions were associated with the earliest of the schemes. The data were accessed using the Carbon Pricing Dashboard. They were last updated on March 31, 2023.

Carbon price and share of greenhouse gas emissions covered by carbon pricing (Figure 2n)

These data were derived from World Bank Group (2023). To estimate the global carbon price, we used the average of the individual scheme prices weighted by the percentage of greenhouse gas emissions covered by each scheme. When multiple schemes covered the same emissions, the emissions were associated with the earliest of the schemes. The data were accessed using the Carbon Pricing Dashboard. They were last updated on March 31, 2023.

Fossil fuel subsidies (Figure 2o)

We obtained data on fossil fuel subsidies between 2010 and 2020 using the International Energy Agency subsidies database (IEA 2022). Fossil fuel consumption subsidies are global totals in 2020 billion US dollars. They cover oil, electricity, natural gas, and coal.

Subsidy values are estimated using the price-gap approach, which involves comparing "average end-user prices paid by consumers with reference prices that correspond to the full cost of supply" (IEA 2022). The subsidy amount is equal to the product of this price gap and the amount consumed (IEA 2022).

Climate emergency declarations (Figure 2p)

We obtained data on climate emergency declarations from the International Climate Emergency Forum (ICEF) "Governments emergency declaration spreadsheet" (Climate Emergency Declaration 2023). These data track governments that have either declared or recognized a climate emergency. The first declaration in the dataset occurred on December 5, 2016. We converted these data to annual totals by considering only cumulative total declarations at the end of each year. For example, the total number of declarations by 2018 corresponds to the number of declarations made prior to December 31, 2018 (including those made in preceding years).

In the manuscript text, we present the number of countries in which one or more jurisdictions have declared a climate emergency. We obtained this information from the International Climate Emergency Forum (ICEF) "Governments emergency declaration spreadsheet" (Climate Emergency Declaration 2023).

Indicators of climate-related responses (Figure 3)

Atmospheric CO_2 (Figure 3a)

We obtained globally averaged monthly estimates of atmospheric CO_2 concentration from NOAA's Global Monitoring Laboratory (Dlugokencky and Tans 2023). Specifically, we used the dataset "Globally averaged marine surface monthly mean data." Note that data for the most recent year are subject to change; potential changes are typically minor. Beginning on February 10, 2021, these CO_2 data are on the WMO X2019 scale. See Global Monitoring Laboratory (2021) for details on the difficulty in attributing a change in atmospheric CO_2 concentration to COVID-19.

Atmospheric methane (Figure 3b)

We obtained globally-averaged monthly estimates of atmospheric methane (CH_4) concentration from NOAA (Ed Dlugokencky, NOAA/ESRL 2023). We used the "Globally averaged marine surface monthly mean data" dataset. These data are derived from measurements made at a global network of sampling sites that were smoothed across time and plotted versus latitude (Dlugokencky et al. 1994, Masarie and Tans 1995). The data are reported as a "dry air mole fraction" (Ed Dlugokencky, NOAA/ESRL 2023).

Atmospheric nitrous oxide (Figure 3c)

We obtained data on nitrous oxide (N_2O) concentration from the NOAA/GML halocarbons program (Dutton et al. 2023). These global monthly mean estimates are measured in parts per billion and are derived by smoothing data collected from a global network of airs sampling sites (Dutton et al. 2023).

Surface temperature anomaly (change) (Figure 3d)

We obtained global monthly mean surface temperature anomaly data from the NASA GISS Surface Temperature Analysis (GISTEMP v4) dataset (GISTEMP Team 2023). We used the "Combined Land-Surface Air and Sea-Surface Water Temperature Anomalies (Land-Ocean Temperature Index, L-OTI)" "Global-mean monthly, seasonal, and annual means" variable. These temperature anomaly/change estimates combine land and ocean surface temperatures. The baseline period used for setting zero is the 1951-1980 mean.

Earth's energy imbalance (Figure 3e)

As an indicator of Earth's energy imbalance, we used global monthly mean TOA All Sky Net Flux estimates from NASA's CERES_EBAF-TOA_Ed4.2 product (Loeb et al. 2018). Roughly, this variable reflects heat accumulation by the Earth; for more details, see Loeb et al. (2018) and

Kato et al. (2018). These data were obtained from the NASA Langley Research Center CERES ordering tool at https://ceres.larc.nasa.gov/data/.

Because this time series has exceptionally high variability, we applied a 12-month running mean smooth. For example, the value in June 2012 corresponds to the average monthly means between July 2011 and June 2012. This was done prior to calculating a loess trendline as described in the "Methods for planetary vital signs" section.

Ocean heat content (Figure 3f)

We obtained yearly (not pentadal) ocean heat content time series data from NOAA's National Centers for Environmental Information (NCEI) (NOAA 2022a). These data are in units of 10^{22} joules and cover the depth range 0-2000 m. The reference period is 1955-2006 (Levitus et al. 2012).

For plotting, we associated each value with the midpoint of the corresponding year (as in the dataset).

Ocean acidity (Figure 3g)

As a proxy for global ocean acidity, we used a time series of seawater pH from the Hawaii Ocean Time-series surface CO2 system data product (HOT 2023). This data product was adapted from Dore et al. (2009). The data were collected at Station ALOHA (22°45'N, 158°00'W). We used the variable "pHmeas_insitu," which is described as the "mean measured seawater pH, adjusted to in situ temperature, on the total scale" (HOT 2023).

Sea level change (Figure 3h)

We obtained data on global mean sea level from GSFC (2021). The variable we used was "GMSL (Global Isostatic Adjustment (GIA) not applied) variation (mm) with respect to 20-year TOPEX/Jason collinear mean reference." According to the dataset description, the "TOPEX/Jason 20 year collinear mean reference is derived from cycles 121 to 858, years 1996-2016" (GSFC 2021). For details, see Beckley et al. (2010) and Beckley et al. (2017).

It should be noted that temperature increase and the warming of the entire ocean is a major contributor to sea-level rise (WCRP Global Sea Level Budget Group 2018).

Minimum Arctic sea ice (Figure 3i)

We obtained minimum Arctic sea ice estimates from Wiese (2019) and NSIDC/NASA (2023). They are derived from satellite observations. For each year, the data indicate the average Arctic sea ice extent for the month of September, which is when the annual minimum occurs. According to NSIDC/NASA (2023), "Arctic sea ice reaches its minimum each September.

September Arctic sea ice is now declining at a rate of 13.1 percent per decade, relative to the 1981 to 2010 average." For plotting purposes, we associated each observation with September 15 (the approximate midpoint of the month).

Greenland ice mass (Figure 3j)

We obtained total land ice mass change measurements for Greenland from Wiese (2019) and NSIDC/NASA (2023). These data show changes in ice sheet mass (in Gt) since April 2002. They come from NASA's GRACE satellites (GRACE and GRACE-FO JPL RL06Mv2 Mascon Solution). The data are in the form of anomalies relative to April 2002. The measurement frequency is roughly monthly. The gap in the data between June 10, 2017 and June 14, 2018 corresponds to the time between missions, and should be kept in mind when interpreting the year-to-date means that we present. For more details on these data, see Watkins et al. (2015).

Antarctica ice mass (Figure 3k)

We obtained total land ice mass change measurements for Antarctica from Wiese (2019). These data show the changes in ice sheet mass (in Gt) since April 2002. They come from NASA's GRACE satellites (GRACE and GRACE-FO JPL RL06Mv2 Mascon Solution). The measurement frequency is roughly monthly. The gap in the data between June 10, 2017 and June 14, 2018 corresponds to the time between missions, and should be kept in mind when interpreting the year-to-date means that we present. For more details on these data, see Watkins et al. (2015).

Cumulative glacier thickness change (Figure 3l)

We obtained cumulative glacier mass balance data from the World Glacier Monitoring Service (WGMS 2022). These data were derived from a database with information about changes in mass, volume, etc. of individual glaciers over time. They are based on averaging over a global set of reference glaciers and are measured relative to 1970.

The units of these data are meters of water equivalent. According to the World Glacier Monitoring Service, "A value of -1.0 [meter of water equivalent] per year is representing a mass loss of 1,000 kg per square meter of ice cover or an annual glacier-wide ice thickness loss of about 1.1 m per year, as the density of ice is only 0.9 times the density of water" (WGMS 2022).

For plotting, we associated each value with the midpoint of the corresponding year.

Total area burned by wildfires in the United States (Figure 3m)

These data come from the National Interagency Coordination Center at The National Interagency Fire Center (National Interagency Coordination Center 2023) and include Alaska and Hawaii. The total for 2004 does not include state lands within North Carolina.

Although wildfire risk depends on many factors including forest management, climate change is likely a significant contributor in the United States (An et al. 2015) and globally (Jolly et al. 2015).

As with global tree cover loss due to fires (figure 3m), this dataset does not distinguish between natural and human-ignited fires.

Global tree cover loss due to fires (Figure 3n)

We obtained global estimates of tree cover loss due to fires from Tyukavina et al. (2022). Tree cover refers to vegetation with height 5 m or greater. These estimates exclude the burning of felled trees, but include both natural and human-ignited fires (Tyukavina et al. 2022).

These data were downloaded using the Global Forest Watch platform (World Resources Institute 2023).

Billion-dollar floods in the United States (Figure 3o)

We obtained data on the frequency of billion-dollar floods in the United States from NOAA (2022b). This dataset covers the number of floods per year (since 1980) with at least 1 billion USD in damages. All damage estimates were CPI-adjusted to 2022 (NOAA 2022b). See Smith (2022) for details.

Climate change is likely associated with increasing flood risk in many parts of the world, although estimates may be highly uncertain (Hirabayashi et al. 2013, Alfieri et al. 2017). Because the data we present relate to economic damages, an increasing trend may be partly due to rising vulnerability, exposure, and GDP (Cardona et al. 2012, Lavell et al. 2012).

Extremely hot days relative to 1961-1990 (Figure 3p)

We used the "TX90p" temperature metric to assess the frequency of extremely hot days (Donat et al. 2013). This variable is derived from the GHCNDEX dataset and indicates the proportion of days where the maximum temperature exceeds the 90th percentile for the baseline period 1961-1990. Thus, it should remain around 10% in the absence of an overall temperature trend. To obtain a single global time series, the gridded spatio-temporal time series were averaged across Earth's surface (from -84 to 84 latitude). For details, see Zhang et al. (2005) and Donat et al. (2013).

Note that climate change has been linked to increases in both the frequency and intensity of extreme heat events (Luber and McGeehin 2008).

Special topics (Figure 5)

Economics (Figure 5a)

This graph is adapted from a similar version presented by WU Vienna (2022). The data originally come from the Global Material Flows Database (UNEP IRP 2023).

Stopping warming (Figure 5b)

The data in this figure come from the State of Carbon Dioxide Removal (CDR) report (Smith et al. 2023).

Specifically, the estimates for land management and novel methods are described as follows: "Almost all current carbon dioxide removal, 2 $GtCO_2$/yr, comes from conventional management of land and a tiny fraction, 0.002 $GtCO_2$/yr, results from novel methods" (Smith et al. 2023, page 8).

According to the report, "In 2050, global scenarios that limit warming to 2°C or lower indicate additional CDR of 4.8 (0.58 to 13) $GtCO_2$ per year, compared with 2020" (Smith et al. 2023, page 86). Adding current (2 $GtCO_2$/yr) and additional required (4.8 $GtCO_2$/yr) CDR gives a total estimate of 6.8 $GtCO_2$/yr needed in 2050, as shown in our figure. However, this estimate is highly uncertain—see Smith et al. (2023) for details.

Stopping coal consumption (Figure 5c)

We obtained estimates of coal emissions by country from version 2022v27 of the Global Carbon Project's fossil CO2 emissions dataset, which includes total emissions by country from 1750 to 2021, where available (Andrew and Peters 2022). For our graph, we considered only three countries with the greatest coal emissions in 2021—China, India, and the United States.

Food security and undernourishment (Figure 5e)

Data on the global prevalence of undernourishment from 2001 to 2022 come from FAOSTAT (FAOSTAT 2023). The full name of the variable we used is "Prevalence of undernourishment (percent) (annual value)," which is part of FAOSTAT's Suite of Food Security Indicators (FAOSTAT 2023).

Justice (Figure 5f)

We mapped vulnerability to climate change using the 2021 ND-GAIN Vulnerability Index, which covers six sectors—"food, water, health, ecosystem service, human habitat, and infrastructure"—and accounts for exposure, sensitivity, and adaptive capacity (Chen et al. 2023)

Supplemental References

Alfieri L, Bisselink B, Dottori F, Naumann G, de Roo A, Salamon P, Wyser K, Feyen L. 2017. Global projections of river flood risk in a warmer world. Earth's Future 5: 171–182.

An H, Gan J, Cho SJ. 2015. Assessing climate change impacts on wildfire risk in the United States. Forests 6: 3197–3211.

Andrew RM, Peters GP. 2022. The Global Carbon Project's fossil CO2 emissions dataset.

Beckley B, Zelensky N, Holmes S, Lemoine F, Ray R, Mitchum G, Desai S, Brown S. 2010. Assessment of the Jason-2 extension to the TOPEX/Poseidon, Jason-1 sea-surface height time series for global mean sea level monitoring. Marine Geodesy 33: 447–471.

Beckley BD, Callahan PS, Hancock III D, Mitchum G, Ray R. 2017. On the "Cal-Mode" correction to TOPEX satellite altimetry and its effect on the global mean sea level time series. Journal of Geophysical Research: Oceans 122: 8371–8384.

Birkel SD. 2023. 'Daily Temperature, SST, & Sea Ice', Climate Reanalyzer. Climate Change Institute, University of Maine, USA.

British Petroleum Company. 2022. BP statistical review of world energy. British Petroleum Company.

Butler RA. 2023. What's the deforestation rate in the Amazon? Mongabay. (13 September 2023; https://rainforests.mongabay.com/amazon/deforestation-rate.html).

Cardona OD, Van Aalst MK, Birkmann J, Fordham M, Mc Gregor G, Rosa P, Pulwarty RS, Schipper ELF, Sinh BT, Décamps H, others. 2012. Determinants of risk: exposure and vulnerability. Pages 65–108 in. Managing the risks of extreme events and disasters to advance climate change adaptation: special report of the intergovernmental panel on climate change. Cambridge University Press.

Carpenter B, Gelman A, Hoffman MD, Lee D, Goodrich B, Betancourt M, Brubaker M, Guo J, Li P, Riddell A. 2017. Stan: A probabilistic programming language. Journal of statistical software 76.

Chen C, Noble I, Hellmann J, Coffee J, Murillo M, Chawla N. 2023. University of Notre Dame global adaptation index country index technical report. ND-GAIN: South Bend, IN, USA.

Cherian R, Quaas J, Salzmann M, Wild M. 2014. Pollution trends over Europe constrain global aerosol forcing as simulated by climate models. Geophysical Research Letters 41: 2176–2181.

Climate Emergency Declaration. 2023. Climate Emergency Declaration. Climate emergency declarations in 2,346 jurisdictions and local governments cover 1 billion citizens. (13 September 2023; https://climateemergencydeclaration.org/climate-emergency-declarations-cover-15-million-citizens/).

Collen B, Loh J, Whitmee S, McRAE L, Amin R, Baillie JE. 2009. Monitoring change in vertebrate abundance: the Living Planet Index. Conservation Biology 23: 317–327.

Copernicus. 2023. Tracking breaches of the 1.5^{0}C global warming threshold. (23 August 2023; https://climate.copernicus.eu/tracking-breaches-150c-global-warming-threshold).

Diamond MS. 2023. Detection of large-scale cloud microphysical changes and evidence for decreasing cloud brightness within a major shipping corridor after implementation of the International Maritime Organization 2020 fuel sulfur regulations. EGUsphere 2023: 1–17.

Dlugokencky E, Steele L, Lang P, Masarie K. 1994. The growth rate and distribution of atmospheric methane. Journal of Geophysical Research: Atmospheres 99: 17021–17043.

Dlugokencky E, Tans P. 2023. NOAA/GML. Trends in Atmospheric Carbon Dioxide. NOAA/GML. (13 September 2023; https://www.esrl.noaa.gov/gmd/ccgg/trends/).

Donat MG, Alexander LV, Yang H, Durre I, Vose R, Caesar J. 2013. Global land-based datasets for monitoring climatic extremes. Bulletin of the American Meteorological Society 94: 997–1006.

Dong B, Sutton RT, Shaffrey L, Harvey B. 2022. Recent decadal weakening of the summer Eurasian westerly jet attributable to anthropogenic aerosol emissions. Nature Communications 13: 1148.

Dutton GS, Hall BD, Dlugokencky EJ, Lan X, Madronich M, Nance JD, Peterson KM. 2023. Combined Atmospheric Nitrous Oxide Dry Air Mole Fractions from the NOAA GML Halocarbons Sampling Network, 1977-2023, Version: 2023-08-30.

Ed Dlugokencky, NOAA/ESRL. 2023. Trends in Atmospheric Methane. Trends in Atmospheric Methane. (13 September 2023; https://www.esrl.noaa.gov/gmd/ccgg/trends_ch4/).

FAOSTAT. 2023. FAOSTAT Database on Agriculture. FAOSTAT Database on Agriculture. (1 June 2023; https://www.fao.org/faostat/en/#home).

Fonnesbeck CJ, Patil A, Huard D, Salvatier J. 2017. PyMC Documentation.

Forster PM, Smith CJ, Walsh T, Lamb WF, Lamboll R, Hauser M, Ribes A, Rosen D, Gillett N, Palmer MD, others. 2023. Indicators of Global Climate Change 2022: annual update of large-scale indicators of the state of the climate system and human influence. Earth System Science Data 15: 2295–2327.

Friedlingstein P, O'Sullivan M, Jones MW, Andrew RM, Gregor L, Hauck J, Le Quéré C, Luijkx IT, Olsen A, Peters GP, others. 2022. Global carbon budget 2022. Earth System Science Data 14: 4811–4900.

GISTEMP Team. 2023. GISS Surface Temperature Analysis (GISTEMP), version 4. NASA Goddard Institute for Space Studies. (13 September 2023; https://data.giss.nasa.gov/gistemp/).

Global Forest Watch. 2022. Assessing Trends in Tree Cover Loss Over 20 Years of Data. (17 August 2022; https://www.globalforestwatch.org/blog/data-and-research/tree-cover-loss-satellite-data-trend-analysis/).

Global Monitoring Laboratory. 2021. Can we see a change in the CO2 record because of COVID-19? Can we see a change in the CO2 record because of COVID-19? (30 April 2021; https://www.esrl.noaa.gov/gmd/ccgg/covid2.html).

GSFC. 2021. Global Mean Sea Level Trend from Integrated Multi-Mission Ocean Altimeters TOPEX/Poseidon, Jason-1, OSTM/Jason-2, and Jason-3 Version 5.1 Ver. 5.1.

Hansen JE, Lacis AA. 1990. Sun and dust versus greenhouse gases: An assessment of their relative roles in global climate change. Nature 346: 713–719.

Hansen JE, Sato M, Simons L, Nazarenko LS, von Schuckmann K, Loeb NG, Osman MB, Kharecha P, Jin Q, Tselioudis G, others. 2022. Global warming in the pipeline. arXiv preprint arXiv:2212.04474.

Hansen MC, Potapov PV, Moore R, Hancher M, Turubanova SA, Tyukavina A, Thau D, Stehman SV, Goetz SJ, Loveland TR, Kommareddy A, Egorov A, Chini L, Justice CO, Townshend JRG. 2013. High-Resolution Global Maps of 21st-Century Forest Cover Change. Science 342: 850-853. Data available on-line from:http://earthenginepartners.appspot.com/science-2013-global-forest. Accessed through Global Forest Watch on 7/13/22. www.globalforestwatch.org.

Hausfather Z, Forster P. 2023. Analysis: How low-sulphur shipping rules are affecting global warming. Carbon Brief. (19 July 2023; https://www.carbonbrief.org/analysis-how-low-sulphur-shipping-rules-are-affecting-global-warming/).

Hirabayashi Y, Mahendran R, Koirala S, Konoshima L, Yamazaki D, Watanabe S, Kim H, Kanae S. 2013. Global flood risk under climate change. Nature Climate Change 3: 816–821.

Hoesly RM, Smith SJ, Feng L, Klimont Z, Janssens-Maenhout G, Pitkanen T, Seibert JJ, Vu L, Andres RJ, Bolt RM, others. 2018. Historical (1750–2014) anthropogenic emissions of reactive gases and aerosols from the Community Emissions Data System (CEDS). Geoscientific Model Development 11: 369–408.

HOT. 2023. Hawaii Ocean Time-series (HOT). Hawaii Ocean Time-series (HOT). (13 September 2023; https://hahana.soest.hawaii.edu/hot/hotco2/hotco2.html).

Huang B, Liu C, Banzon V, Freeman E, Graham G, Hankins B, Smith T, Zhang H-M. 2021. Improvements of the daily optimum interpolation sea surface temperature (DOISST) version 2.1. Journal of Climate 34: 2923–2939.

IEA. 2022. Energy subsidies: Tracking the impact of fossil-fuel subsidies. International Energy Agency.

IMF. 2022. World Economic Outlook Database: April 2022 Edition. International Monetary Fund.

IPCC. 2018. Global Warming of 1.5° C: An IPCC Special Report on the Impacts of Global Warming of 1.5° C Above Pre-industrial Levels and Related Global Greenhouse Gas Emission Pathways, in the Context of Strengthening the Global Response to the Threat of Climate Change, Sustainable Development, and Efforts to Eradicate Poverty. Intergovernmental Panel on Climate Change.

IPCC. 2021. Climate Change 2021: The Physical Science Basis. Contribution of Working Group I to the Sixth Assessment Report of the Intergovernmental Panel on Climate Change [Masson-Delmotte, V., P. Zhai, A. Pirani, S. L. Connors, C. Péan, S. Berger, N. Caud, Y. Chen, L. Goldfarb, M. I. Gomis, M. Huang, K. Leitzell, E. Lonnoy, J. B. R. Matthews, T. K. Maycock, T. Waterfield, O. Yelekçi, R. Yu and B. Zhou (eds.)]. Cambridge University Press.

Jolly WM, Cochrane MA, Freeborn PH, Holden ZA, Brown TJ, Williamson GJ, Bowman DM. 2015. Climate-induced variations in global wildfire danger from 1979 to 2013. Nature communications 6: 1–11.

Kato S, Rose FG, Rutan DA, Thorsen TJ, Loeb NG, Doelling DR, Huang X, Smith WL, Su W, Ham S-H. 2018. Surface irradiances of edition 4.0 clouds and the earth's radiant energy system (CERES) energy balanced and filled (EBAF) data product. Journal of Climate 31: 4501–4527.

Lavell A, Oppenheimer M, Diop C, Hess J, Lempert R, Li J, Muir-Wood R, Myeong S, Moser S, Takeuchi K, others. 2012. Climate change: new dimensions in disaster risk, exposure, vulnerability, and resilience. Pages 25–64 in. Managing the risks of extreme events and disasters to advance climate change adaptation: Special report of the intergovernmental panel on climate change. Cambridge University Press.

Loeb NG, Doelling DR, Wang H, Su W, Nguyen C, Corbett JG, Liang L, Mitrescu C, Rose FG, Kato S. 2018. Clouds and the earth's radiant energy system (CERES) energy balanced and filled (EBAF) top-of-atmosphere (TOA) edition-4.0 data product. Journal of Climate 31: 895–918.

Loeb NG, Johnson GC, Thorsen TJ, Lyman JM, Rose FG, Kato S. 2021. Satellite and ocean data reveal marked increase in Earth's heating rate. Geophysical Research Letters 48: e2021GL093047.

Loh J, Green RE, Ricketts T, Lamoreux J, Jenkins M, Kapos V, Randers J. 2005. The Living Planet Index: using species population time series to track trends in biodiversity. Philosophical Transactions of the Royal Society B: Biological Sciences 360: 289–295.

Luber G, McGeehin M. 2008. Climate change and extreme heat events. American journal of preventive medicine 35: 429–435.

Masarie KA, Tans PP. 1995. Extension and integration of atmospheric carbon dioxide data into a globally consistent measurement record. Journal of Geophysical Research: Atmospheres 100: 11593–11610.

McRae L, Deinet S, Freeman R. 2017. The diversity-weighted living planet index: controlling for taxonomic bias in a global biodiversity indicator. PloS one 12: e0169156.

National Interagency Coordination Center. 2023. National Interagency Fire Center. National Interagency Fire Center. (13 July 2023; https://www.nifc.gov/fireInfo/fireInfo_stats_totalFires.html).

Natural Resources Canada. 2023. Fire M3 Hotspots. (7 July 2023; https://cwfis.cfs.nrcan.gc.ca/maps/fm3).

NOAA. 2022a. National Centers for Environmental Information: Global Ocean Heat and Salt Content. Global Ocean Heat and Salt Content. (15 June 2023; https://www.nodc.noaa.gov/OC5/3M_HEAT_CONTENT/).

NOAA. 2022b. National Centers for Environmental Information (NCEI) U.S. Billion-Dollar Weather and Climate Disasters. (https://www.ncei.noaa.gov/access/monitoring/billions/).

NSIDC/NASA. 2023. Global Climate Change: Vital Signs of the Planet. Vital Signs of the Planet. (13 September 2023; https://climate.nasa.gov/).

O'Rourke PR, Smith SJ, Mott A, Ahsan H, McDuffie EE, Crippa M, Klimont Z, McDonald B, Wang S, Nicholson MB, Feng L, Hoesly RM. 2021. CEDS v_2021_02_05 Release Emission Data.

Our World in Data. 2023. Data Explorer: Air Pollution. (27 June 2023; https://ourworldindata.org/explorers/air-pollution).

Persad GG, Samset BH, Wilcox LJ. 2022. Aerosols must be included in climate risk assessments. Nature 611: 662–664.

Ripple WJ, Wolf C, Newsome TM, Barnard P, Moomaw WR. 2020. World scientists' warning of a climate emergency. BioScience 70: 8–12.

Rousi E, Kornhuber K, Beobide-Arsuaga G, Luo F, Coumou D. 2022. Accelerated western European heatwave trends linked to more-persistent double jets over Eurasia. Nature communications 13: 1–11.

Saha S, Moorthi S, Wu X, Wang J, Nadiga S, Tripp P, Behringer D, Hou Y-T, Chuang H, Iredell M, others. 2014. The NCEP climate forecast system version 2. Journal of climate 27: 2185–2208.

Salzmann M. 2016. Global warming without global mean precipitation increase? Science advances 2: e1501572.

Smith AB. 2022. 2021 U.S. billion-dollar weather and climate disasters in historical context. (4 May 2022; https://www.climate.gov/news-features/blogs/beyond-data/2021-us-billion-dollar-weather-and-climate-disasters-historical).

Smith SM, Geden O, Nemet G, Gidden M, Lamb WF, Powis C, Bellamy R, Callaghan M, Cowie A, Cox E, Fuss S, Gasser T, Grassi G, Greene J, Lück S, Mohan A, Müller-Hansen F, Peters G, Pratama Y, Repke T, Riahi K, Schenuit F, Steinhauser J, Strefler J, Valenzuela JM, Minx JC. 2023. The State of Carbon Dioxide Removal–1st Edition. The State of Carbon Dioxide Removal.

Stendel M, Francis J, White R, Williams PD, Woollings T. 2021. The jet stream and climate change. Pages 327–357 in. Climate Change. Elsevier.

Stott PA, Allen M, Christidis N, Dole RM, Hoerling M, Huntingford C, Pall P, Perlwitz J, Stone D. 2013. Attribution of weather and climate-related events. Pages 307–337 in. Climate science for serving society. Springer.

Strauss BH, Orton PM, Bittermann K, Buchanan MK, Gilford DM, Kopp RE, Kulp S, Massey C, de Moel H, Vinogradov S. 2021. Economic damages from Hurricane Sandy attributable to sea level rise caused by anthropogenic climate change. Nature communications 12: 1–9.

The Energy Institute. 2023. Statistical Review of World Energy. The Energy Institute.

The World Bank. 2023a. Fertility rate, total (births per woman). (14 June 2023; https://data.worldbank.org/indicator/SP.DYN.TFRT.IN).

The World Bank. 2023b. GDP (constant 2015 US$). (14 June 2023; https://data.worldbank.org/indicator/NY.GDP.MKTP.KD).

The World Bank. 2023c. Air transport, passengers carried. (14 June 2023; https://data.worldbank.org/indicator/IS.AIR.PSGR).

Trenberth KE, Fasullo JT, Shepherd TG. 2015. Attribution of climate extreme events. Nature Climate Change 5: 725–730.

Tyukavina A, Potapov P, Hansen MC, Pickens AH, Stehman SV, Turubanova S, Parker D, Zalles V, Lima A, Kommareddy I, others. 2022. Global Trends of Forest Loss Due to Fire From 2001 to 2019. Frontiers in Remote Sensing 3: 825190.

UNEP IRP. 2023. United Nations Environment Programme, International Resource Panel, Global Material Flows Database.

VISHOP. 2023. Sea Ice Extent [million km2]. (24 June 2023; https://ads.nipr.ac.jp/vishop/#/extent).

Wall CJ, Norris JR, Possner A, McCoy DT, McCoy IL, Lutsko NJ. 2022. Assessing effective radiative forcing from aerosol–cloud interactions over the global ocean. Proceedings of the National Academy of Sciences 119: e2210481119.

Watkins MM, Wiese DN, Yuan D-N, Boening C, Landerer FW. 2015. Improved methods for observing Earth's time variable mass distribution with GRACE using spherical cap mascons. Journal of Geophysical Research: Solid Earth 120: 2648–2671.

WCRP Global Sea Level Budget Group. 2018. Global sea-level budget 1993–present. Earth System Science Data 10: 1551–1590.

WGMS. 2022. The World Glacier Monitoring Service. (3 May 2022; https://wgms.ch/global-glacier-state/).

Wiese D, Yuan D, Boening C, Landerer F, Watkins M. 2019. JPL GRACE and GRACE-FO Mascon Ocean, Ice, and Hydrology Equivalent Water Height RL06M CRI Filtered Version 2.0, Ver. 2.0. PO.DAAC, CA, USA.

World Bank Group. 2023. State and Trends of Carbon Pricing 2023. World Bank, Washington, DC.

World Resources Institute. 2023. Global Forest Watch. (13 July 2023; https://www.globalforestwatch.org/).

Wu L, Zhao H, Wang C, Cao J, Liang J. 2022. Understanding of the effect of climate change on tropical cyclone intensity: a review. Advances in Atmospheric Sciences 39: 205–221.

WU Vienna. 2022. Material flows by material group, 1970-2019. Visualisation based upon the UN IRP Global Material Flows Database. Vienna University of Economics and Business.

WWF. 2022. Living Planet Report 2022 – Building a nature positive society. WWF.

Zhang X, Hegerl G, Zwiers FW, Kenyon J. 2005. Avoiding inhomogeneity in percentile-based indices of temperature extremes. Journal of Climate 18: 1641–1651.

Zhao S, Suzuki K. 2021. Exploring the impacts of aerosols on ITCZ position through altering different autoconversion schemes and cumulus parameterizations. Journal of Geophysical Research: Atmospheres 126: e2021JD034803.

Zheng Y, Zhang Q, Tong D, Davis SJ, Caldeira K. 2020. Climate effects of China's efforts to improve its air quality. Environmental Research Letters 15: 104052.